Synthetic strategy of porous ZnO and CdS nanostructures doped ferroelectric liquid crystal and its optical behavior

Kaushik Pal , Uday Narayan Maiti , Tapas Pal Majumder , Subhas Chandra Debnath , Noureddine Bennis , Jose Manuel Otón

HIGHLIGHTS

- CTAB assisted CdS nanowires prepared having uniform diameter of 65 nm.
- Hydrazine monohydrate assisted ZnO nanorods having uniform length of 2000–4000 nm.
- The mixed band gap of CdS–Felix is increased by $\Delta E_g = 0.35$ eV.
- The mixed band gap of ZnO–Felix is decreased by $\Delta E_g = -0.22$ eV.
- Interesting features from photoluminescence behavior of such hybrid structure.

ABSTRACT

A simple and scalable chemical approach has been proposed for the generation of 1-dimensional nanostructures of two most important inorganic materials such as zinc oxide and cadmium sulfide. By controlling the growth habit of the nanostructures with manipulated reaction conditions, the diameter and uniformity of the nanowires/nanorods were tailored. We studied extensively optical behavior and structural growth of CdS NWs and ZnO NRs doped ferroelectric liquid crystal Felix-017/100. Due to doping band gap has been changed and several blue shifts occurred in photoluminescence spectra because of nanoconfinement effect and mobility of charges.

1. Introduction

Various fabrications of semiconducting materials like cadmium sulfide (CdS) and zinc oxide (ZnO) have attracted much attention to the researchers over the past decades because of their synthesis procedure and functional behavior having unusual optical, electric properties and potential applications [1–3] in nanodevices [4]. Among metal chalcogenides, CdS has been one of the most studied due to its extensive applications in photoelectric conversion in solar cells and light-emitting diodes in flat panel displays [5,6]. CdS nanowires have been synthesized by several techniques. For instance, the growth of thin CdS nanowires (20 nm thick) has been achieved by laser ablation or chemical vapor deposition (CVD) process based on a gold nanocluster catalyzed vapor–liquid–solid (VLS) growth mechanism [7,8]. One-dimensional (1D) specimens such as wires, rods, belts, and tubes falls into the range from 1 to 100 nm and have become the focus of intensive research, owing to their unique applications in mesoscopic physics and fabrication of nanoscale devices. In particular, semiconductor nanowires have stimulated intensive research interest and nanoelectronic applications [9]. Recently, much progress has been made in applications of nanodevices using semiconductor nanowires as building blocks [10]. In this paper we utilize a very simple hydrothermal route to fabricate CdS nanowires with uniform distribution in high yield by using a surfactant.

ZnO is of interest for low-voltage and short wavelength electro-optical devices such as light emitting diodes and diode lasers due to its wide band gap (3.2 eV) and large exciton binding energy of 60 meV [11]. Many ZnO interesting nanostructures including nanobelts, nanobridges, nanonails, and nanoribbons have been fabricated by thermal evaporation of oxide powders [12–15]. Recently, many researchers synthesized ZnO nanowires and nanorods by a

solvothermal process [16,17]. However, the solvothermal process implies the use of toxic, dangerous, and expensive solvents such as amines. As for ZnO nanorods, it is also necessary to prepare them at a high temperature of 180 °C for 24 h using an excellent capping reagent like hydrazine amine which controls the growth of nanorods. The mechanism for the hydrazine assisted hydrothermal synthesis of rodlike ZnO has been presented in the experimental Section 2.

The stable and uniform alignment of liquid crystals (LCs) on a macroscopic scale is essential for the fabrication of high-quality liquid crystal displays (LCDs). Typically, alignment involves modification of a solid substrate that interfaces with the LC. The substrate has some anchoring action resulting in either planar (tangential) or homeotropic (perpendicular) orientation of the LC director (symmetry axis) with respect to the interface [18]. However, the details of LC alignment are not well understood [19–21]. Thus, the search for more easily quantified alignment materials continues. In this paper we have tested doping of ferroelectric liquid crystal Felix-107/100 with different nanomaterials such as CdS and ZnO nanowires/nanorods. We have performed a comparative study of optical properties with pure nanomaterials.

Early investigations observed that the hydrolysis of tetraethyl orthosilicate (TEOS, $Si(OC_2H_5)_4$) under acidic conditions yielded SiO_2 in the form of a glass-like material. Sol–gel derived porous SiO_2 xerogel film is particularly attractive among various low k dielectric candidates in advanced semiconductor devices because of its inherent ultra-low permittivity and high thermal stability through the incorporation of micropores into the SiO_2 skeletal network. So far, most of mesoporous SiO_2 films were prepared by dip-coating methods. However, the rapid evaporation of volatile components followed by dip-coating step will lead to severe concentration gradients across the film. As a result, the mesophase often varies across the films and the calcined films are apt to peel off. Those problems might be overcome to a certain degree by introducing a spin coating method instead of dip-coating step [22,23].

Quite recently, a number of researchers have worked with various nanostructured materials based on sol–gel process and deposited SiO_2 coated film by spin-coating technique. In this paper, we introduce ferroelectric liquid crystal Felix deposited over SiO_2 coated films doped with nanostructured materials such as CdS and ZnO. We have carried out a comparative study of homogeneous LC doping with different nanomaterials. We have focused on comparisons of UV–Vis and photoluminescence spectra, since remarkable differences are shown for different dopants.

2. Experimental

In an earlier publication we obtained a uniform speed of coating for CdS doped FLC matrix [23]. By using that speed as an optimum we have coated all films for further studies.

All chemicals employed in this work were of analytical grade, commercially available and used without further purification. The chemicals such as ethylenediamine (EDA), $Cd(CH_3COO)_2{\cdot}2H_2O$ and sulphur (S) powder, sodium hydroxide pallets, cetyltrimethylammonium bromide (CTAB), Na_2SO_4, hydrazine monohydrate (80% v/v) were used as starting ingredients for synthesis of various types of nanostructured molecules. Those molecules were purchased from Atlanta drugs chemical reagent Co. Ltd. (Merck). 0.35 g of surfactant CTAB with 40 ml solvent EDA were used for different nanostructures preparation. For silica gel preparation, TEOS and Pluronic F127 from Sigma Aldrich were used and HCl (35% of 11.32 M concentrate) and ethanol were obtained from Merck and China, respectively.

2.1. Synthesis of CdS nanowires

In a typical procedure, 0.5 g of $Cd(Ac)_2$ and 0.08 g of S powder were put into 50 ml beaker, dissolved into 40 ml of ethylenediamine under vigorous stirring for 15 min. Then the prepared green coloured solution gradually turned into yellow. During stirring, 0.35 g of CTAB was added into the yellow precursor and wait for 20 min. After complete stirring, the final solution was transferred to a 50 ml Teflon-lined stainless steel autoclave. The autoclave was placed in a heating chamber at 130–180 °C for 4.30 h. Subsequently, the system was allowed to cool down to room temperature naturally. The resulting sample was filtered off and warmed out in a vacuum chamber at 65 °C for 4 h followed by washing with heavy flow of 1 l deionised distilled water and ethanol for several

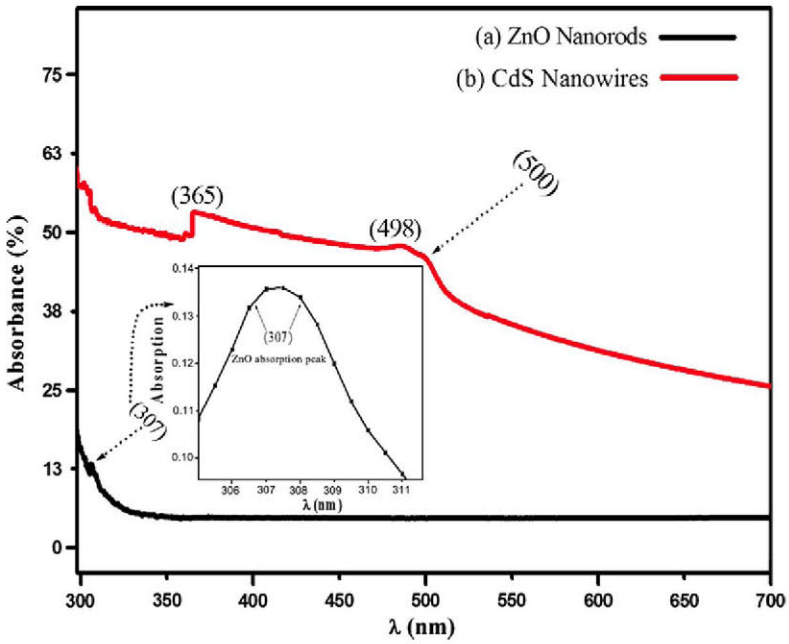

Fig. 1. UV–Vis absorption spectra of CdS nanowires and ZnO nanorods deposited on SiO_2 coated glass substrate.

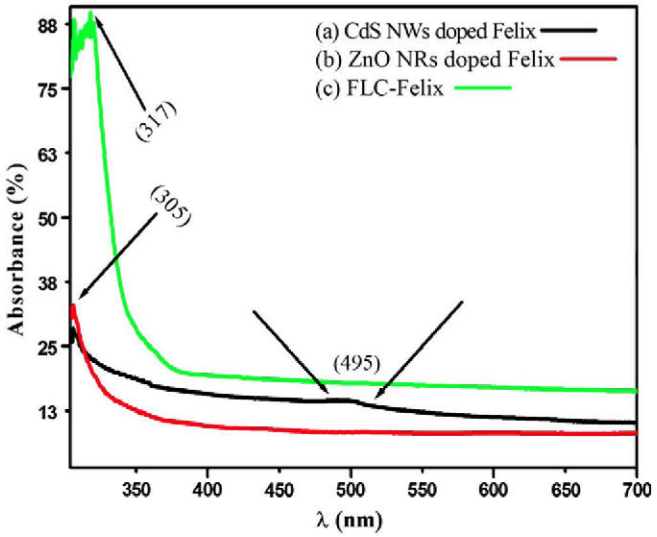

Fig. 2. UV–Vis absorption spectra of Felix doped CdS nanowires and ZnO nanorods deposited on SiO_2 coating glass substrate.

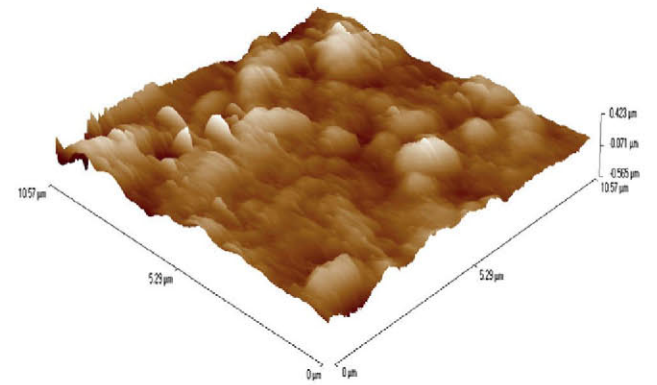

Fig. 3. Atomic force micrograph (AFM) of pure CdS nanostructures on SiO_2 deposited glass substrates.

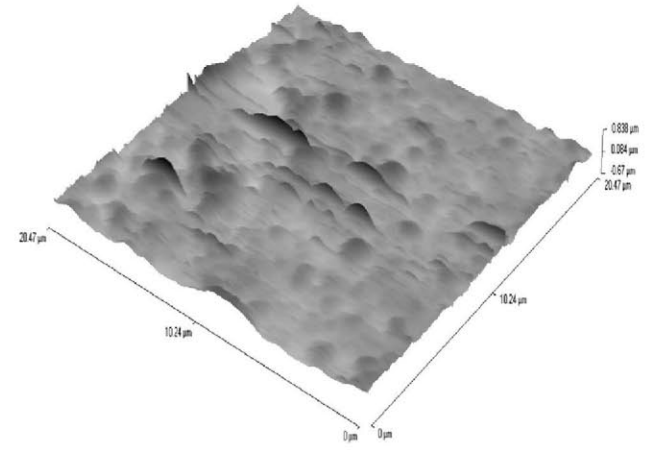

Fig. 4. Atomic force micrograph (AFM) of pure ZnO nanostructures on SiO_2 deposited glass substrates.

times until the produced impurity washed away and separated from the desired sample.

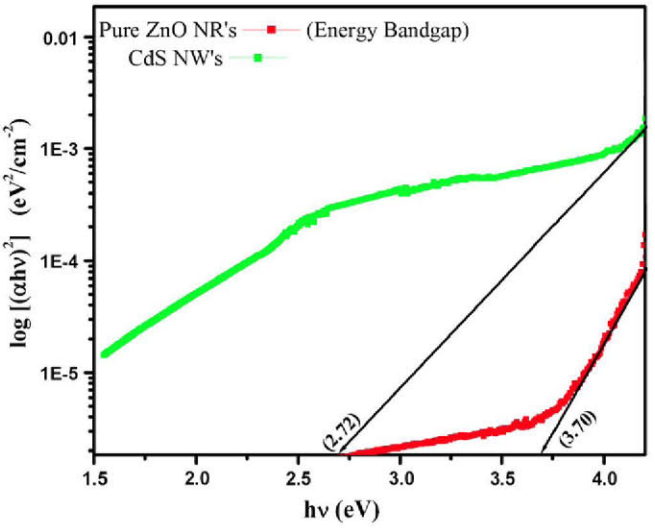

Fig. 5. Evolution of ln $[(\alpha h\nu)^2]$ plotted against photon energy of energy band diagram of pure CdS NWs and ZnO NR's deposited on SiO_2 coated film.

2.2. Synthesis of ZnO nanorods

In a typical synthesis procedure of ZnO nanorods, 0.65 g of $Zn(NO_3)_2{\cdot}6H_2O$, 0.15 g of Na_2SO_4, were loaded into a Teflon-lined stainless steel autoclave with 50 ml capacity and dissolved in 30 ml of deionized water. Then, 5.0 ml of hydrazine monohydrate (80% v/v) solution was added dropwise with vigorous stirring in a magnetic stirrer (REMI). Next, the autoclave was filled with deionized water up to 80% of the total volume. After 10 min stirring, the system was sealed and maintained at 180 °C for 24 h. When the system became cool at room temperature naturally, the resulted precipitation was collected by filtration and washed with absolute ethanol and distilled water in sequence for several times. The final product was dried in a vacuum chamber at 50 °C for 4 h. A brownish powder was obtained and this powder was annealed at 600 °C for 1.5 h.

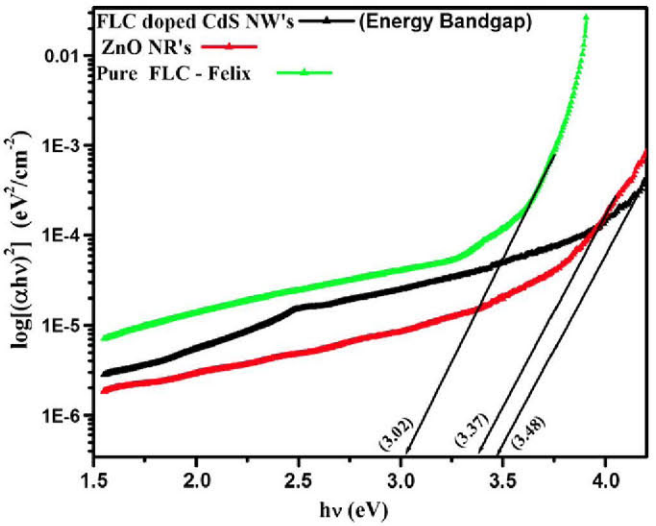

Fig. 6. Evolution of ln $[(\alpha h\nu)^2]$ plotted against photon energy of energy band diagram of Felix doped CdS NW's and ZnO NR's deposited on SiO_2 coated film.

2.3. Mechanism of chemical reactions synthesis of CdS/ZnO nanowires/ nanorods

In this hydrothermal reaction, ethylenediamine (en) acted as a solvent as well as a complexing agent. In our synthetic system, the investigation of CdS nanoparticles formation indicated that the nucleation and growth were well controlled. Firstly, ethylenediamine, as a strongly bidentating solvent, was ready to form relatively stable Cd^{2+} complexes [24,25]. Next, cadmium ions could combine with an ethylenediamine molecule, which acted as a bidentate ligand, to form a Cd–ethylenediamine complex ($[Cd(en)_2]^{2+}$) [26] and that is stabilized in the solution. Meanwhile, S powder was dissolved in ethylenediamine. Finally, due to slow release of S^{2-} ions and the low free Cd^{2+} concentration ($\log\beta_2 = 10.09$, β_2 is the stability constant of the complex ($[Cd(en)_2]^{2+}$), the reaction rate is slow, which is in favor of the oriented growth of the CdS nanowires [27].

Cd^{+2} + EDA molecules(acting as a bidentate ligand)

$\leftrightarrow$ ($[\mathbf{Cd}(\mathbf{en})_2]^{2+}$)[Cd-ethylenediamine complex]

In ZnO nanorod synthesis procedure, we introduced Zn^{2+} aqueous solution and then $Zn(OH)_2$ colloids form, according to

$$Zn^{2+} + 2OH^- \leftrightarrow Zn(OH)_2 \quad (1)$$

If the pH value in the aqueous solution is about 11 then $Zn(OH)_2$ is the main composition. Then, during the hydrothermal process, part of the $Zn(OH)_2$ colloids dissolves into Zn^{2+} and OH^- according to reaction (2). When the concentration of Zn^{2+} and OH^- reaches the super saturation degree of ZnO, then ZnO nuclei will form according to reaction (3). Thus, the growth units of $[Zn(OH)_4]^{2-}$ form according to reaction (4):

$$Zn(OH)_2 \leftrightarrow Zn^{2+} + 2OH^- \quad (2)$$

$$Zn^{2+} + 2OH^- \leftrightarrow ZnO + H_2O \quad (3)$$

$$Zn(OH)_2 + 2OH^- \leftrightarrow [Zn(OH)_4]^{2-} \quad (4)$$

2.4. Preparation of silicate sol and spin coating on glass substrate

To prepare Si-Sol, tetraethylorthosilicate (TEOS) was added to the mixed solution of HCl, ethanol and H_2O and the prepared solution was heated at 60 °C for 1.30 h with stirring. This pre-hydrolyzed solution was then added dropwise to the dissolved Pluronic F127 in ethanol while stirring. In this typical experiment, the molar ratio for the chemical composition of Si- Sol was as follows: TEOS:F127:HCl:H_2O:EtOH = 1:0.009:0.2:9.2:30 [22,23].

The entire prepared initial sols was aged with stirring at room temperature for 3 h, before they were spin coated using APEX SCU-2008C spin coater, on cleaned glass substrates with acetone solution. The spin speed was adjusted to 1000 rpm with spinning time of 20 s. The coated films were then aged at 25 °C for three days in a closed chamber under relative humidity (RH), which was controlled with saturated salt solution. To remove the surfactant from coated SiO_2 films, those glass substrates were carried out by heating rate of 1 °C/min to reach at 150 °C for 3 h at the peak temperature.

2.5. Hybrid nano composite and thin film preparation

Pyrex glass substrates (2.5 cm × 3 cm) were cleaned and washed with deionized distilled water and then with acetone vapor. To prepare nano composite, the desired amount of CdS (0.05142 g) NWs and ZnO (0.068 g) NRs doped with 0.01749 g of ferroelectric liquid crystal (Felix-017/100), which was dissolved into 5 ml ethanol with each amount of nanomaterials. Those prepared solution ultrasonically mixed under slight heating for 30 min, for which CdS and ZnO nanomaterials completely dispersed with proper amount of Felix, which was taken previously. The obtained films were then dried under ambient condition in hot plate.

Field emission scanning electron microscopy (FE-SEM) measurements were carried out on a S4800 at 5.0 kV to get SEM micrograph of the studied composition. The SEM measurement on the SiO_2 coated glass substrate for LC and nanodoped (CdS nanowires) LC carried out on at 18 kV, Jadavpur University. A UV–Vis spectrophotometer (UV-2401 PC, Shimadzu, Japan, IACS), was used to record the electronic absorption spectra of the films at room temperature. Photoluminescence spectra were measured at room temperature with a PerkinElmer LS55 Fluorescence spectrometer using excitation source of 325 nm and 425 nm line of a He–Cd laser.

3. Results and discussion

Ultraviolet visible (UV/Vis) absorption spectra of CdS and ZnO nanostructured thin films deposited on SiO_2 coated pyrex glass substrate at room temperature show that the fundamental

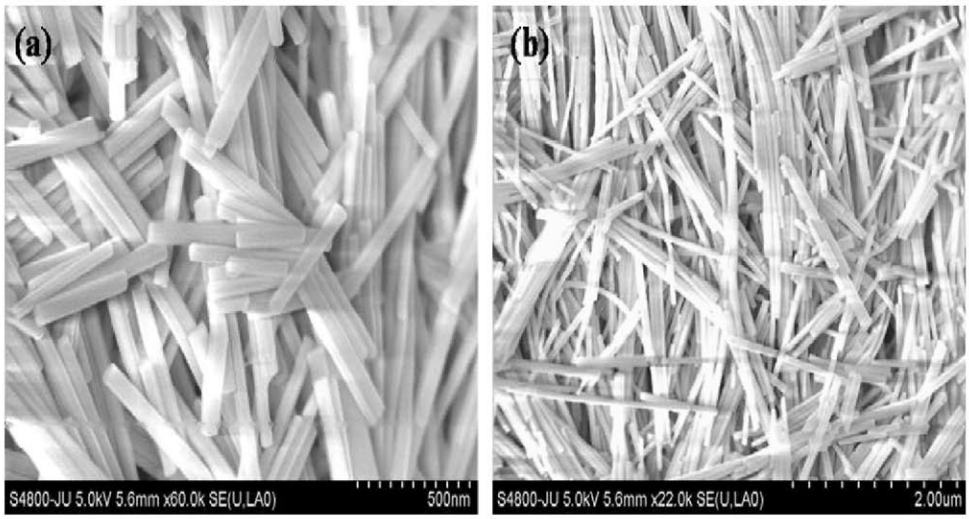

Fig. 7. FE-SEM images of CdS nanowires evolved in addition of CTAB. (a) 2 μm and (b) 500 nm microscopic resolution.

absorbance edge are blue shifted from 350 to 300 nm in comparison to FLC–Felix doped with those previously obtained nano materials. The sharp absorption peak maxima are found at 365 nm and 498 nm with a clear shoulder hump generated at 500 nm due to CdS nanowires. According to UV absorption spectrua of ZnO nanorods, there is no such typical sharp peak appeared for it except a small hump at 307 nm region as shown in inset of Fig. 1. That is clearly depicting with dotted arrow. In addition, we investigate absorption band structure under suitable proportion of Felix doped CdS and ZnO nanomaterials shown in Fig. 2. There is no such distinct absorption peak maxima found in blue shift region from 350 to 300 nm except a small hump appeared at 305 nm of same wavelength region corresponds to Felix doped ZnO NRs and CdS NWs as shown by arrow. While, a broad shoulder peak is located at 495 nm, which signifies due to Felix incorporation with CdS NWs. In addition to this, absorption band maxima are shifted at 317 nm due to pure FLC–Felix deposition on SiO_2 coated glass substrate.

The thickness of films is ranging from 0.494 μm to 0.754 μm (Figs. 3 and 4), as observed from the surface morphology from atomic force microscopic measurement (AFM) of CdS and ZnO nanostructured thin films deposited on SiO_2 coated glass substrates.

We calculated the optical band gap, E_g from UV/Vis absorption spectra with the help of the following equation as given below [28]:

$$\alpha h\nu = A(h\nu - E_g)^p$$

Where, A is a constant related to the effective masses associated with the bands. $p = 1/2$ for a direct band gap material, 2 for an indirect band gap material and 3/2 for a forbidden–direct energy gap and the estimated E_g values are in the range from 2.40 to 2.42 eV for CdS materials [29] and for nanostructured CdS, respectively [30] as reported earlier. The band gap of ZnO is 3.44 eV at low temperatures and 3.37 eV at room temperature as reported earlier [31,32], which corresponds to emission in the UV region. We obtained the band gap of nanowires for pure CdS = 2.72 eV and pure ZnO = 3.70 eV (Fig. 5). Therefore, the obtained band gap of pure CdS and ZnO nanowires are changed due to quantum confinement effect. It may be shifted due to the introduction of some silicate coating over glass slides. We also obtained the band gap of nanodoped Felix such as 3.02 eV for pure Felix FLC, 3.48 eV for CdS nanostructures doped Felix FLC and 3.37 eV for ZnO nanostructures doped Felix FLC (Fig. 6). Due to introduction of CdS nanostructures in Felix, the band gap due to doping is increased by ΔE_g (CdS–Felix) = 0.35 eV. Such increase is definitely due to the confinement effect of charges in the system. But due to the introduction of ZnO nanostructures in Felix, the band gap due to doping is decreased by ΔE_g (ZnO–Felix) = −0.22 eV. Such decrease may be due to the increase of mobility of charges between ZnO and Felix in the confined geometry. ZnO has itself low ionic conductivity compared to CdS, so the band gap decreases for ZnO doped Felix may be due to the increase of ionic conductivity in such system as a whole, but for CdS doped Felix band gap decreases due to the decrease of degrees of freedom in the system as a whole.

The CdS nanowires are of high uniformity and high yield with the addition of a certain concentration of the surfactant CTAB in the hydrothermal method (Fig. 7a). The length of those nanowires is up to several nanometers. The nanowires have diameters at the order of 65 nm, which is uniform along the entire nanowires length (Fig. 7b). Therefore, 0.01542 g of CdS nanowires with 65 nm diameter mixed with 4 ml of ethanol and then doped it with 0.01749 g of Felix–FLC was used to obtain good uniform CdS nanowires. Then the mixed compositions were spin coated on SiO_2 coating glass substrate.

FE-SEM micrographs show ZnO nanorods structural growth with diameter 483 nm before annealed (Fig. 8a and b). The wide diameter of ZnO nanorods varies from 576 nm to 900 nm. We observe non uniformity to their length distribution in the range of several micrometer of the order of 2–4 μm after annealed it over 600 °C at 1.5 h and some porous like structures all over the surface of nanorods depicted in Fig. 8c. For thin film preparation, ZnO NRs ultrasonically mixed with ethanol and proper amount of LC–Felix with slightly heating under ultrasonic vibration until ZnO nanomaterials completely dispersed with Felix to form ZnO nanocomposite.

When only LC–Felix is spin coated on SiO_2 coated polyimide films then most of the grains are oriented in a peculiar growth on the substrate forming flower like structures as shown in SEM images (Fig. 9a and b). Higher resolution SEM images (Fig. 9c) illustrated microflower like structural growth of nano composites and that obtained due to the dispersion of CdS NWs in Felix. Higher magnified SEM image (Fig. 9d) clearly indicated CdS nanowires distributed on SiO_2 coated polyimide film.

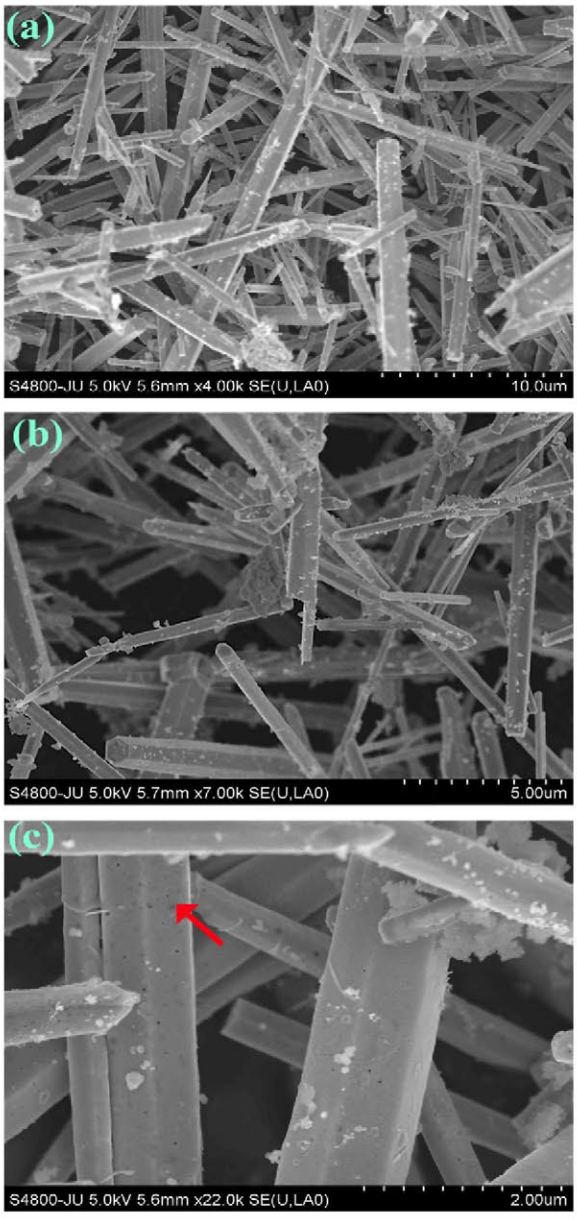

Fig. 8. FE-SEM images of ZnO nanorods (a) 10 μm, (b) 5 μm microscopic resolution before annealed and (c) porous surface ZnO nanorods, 10 μm microscopic resolution annealed at 600 °C for 1.5 h.

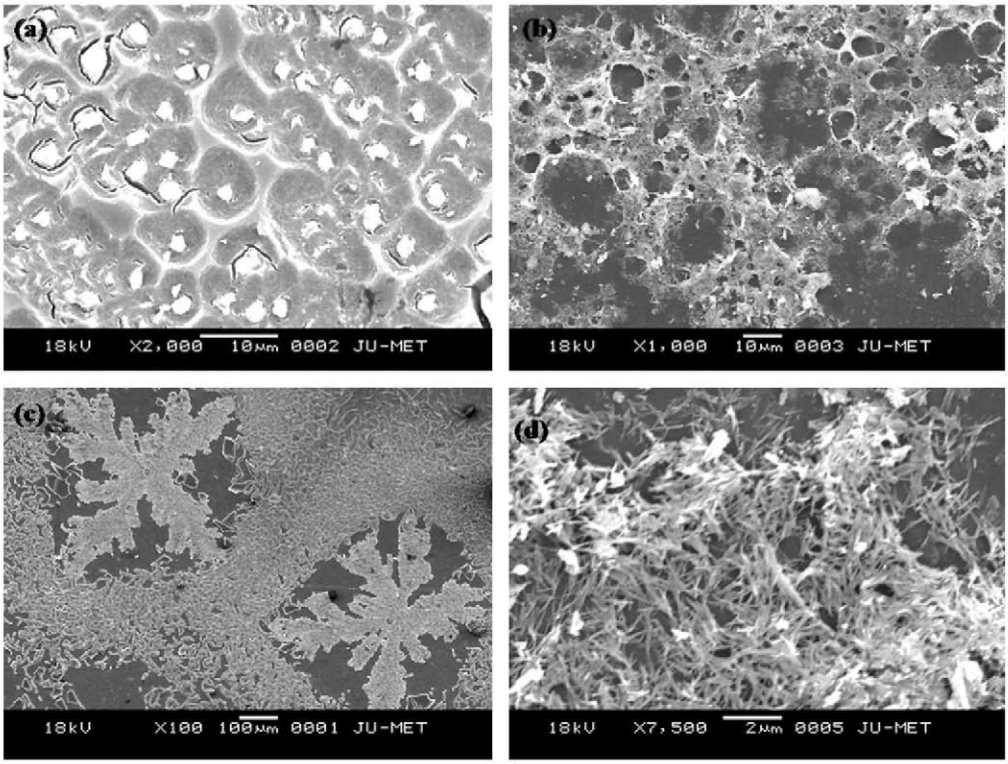

Fig. 9. SEM images of (a) and (b), Felix (FLC) deposited on SiO_2 coated Polyimide film. SEM images of (c) micro-flower structural growth formation when Felix completely dispersed with CdS NWs under ultrasonic vibration of slight heating (d) before ultrasonication, CdS nanowires distributed on SiO_2 coated Polyimide film.

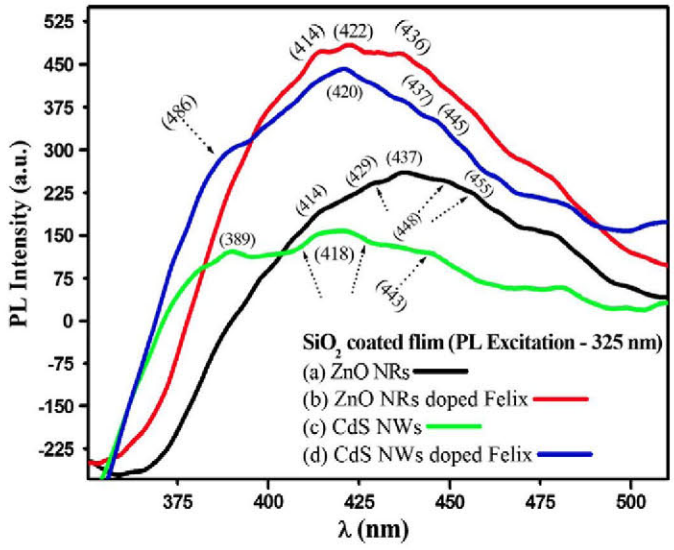

Fig. 10. Photoluminescence spectra of (a) ZnO NRs, (b) ZnO NRs doped Felix, (c) CdS NWs and (d) CdS NWs doped Felix, deposited on SiO_2 coated thin film on glass substrates at excitation wavelength, 325 nm.

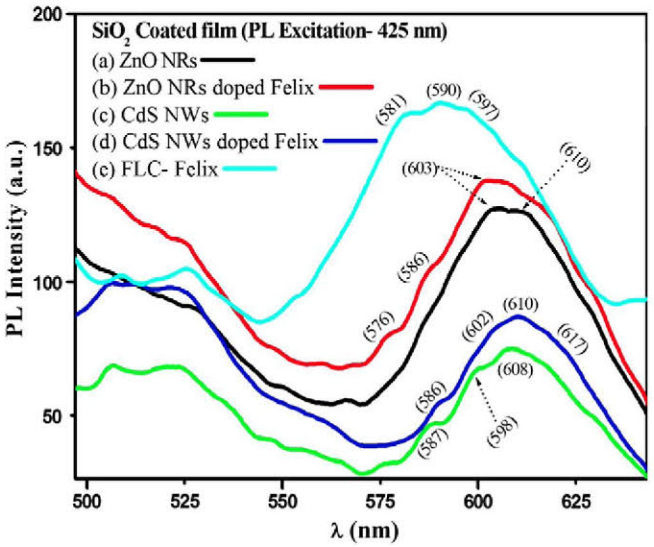

Fig. 11. Photoluminescence spectra of (a) ZnO NRs, (b) ZnO NRs doped Felix, (c) CdS NWs and (d) CdS NWs doped Felix, deposited on SiO_2 coated thin film on glass substrates at excitation wavelength, 425 nm.

The photoluminescence (PL) spectra were recorded at excitation wavelength of 325 nm and 425 nm of prepared ZnO NRs and CdS NWs corresponds to those nano composite (nanodoped Felix) measured at room temperature as shown in Figs. 10 and 11, respectively. For CdS NWs (Fig. 10c, a broad luminescence peak is located at 418 nm region with distinct shoulder hump of violet emission peak on the left hand side at 389 nm and right hand side at 443 nm wavelength region corresponds to CdS nanowires. For ZnO NRs (Fig. 10a), a high intense strong emission peak is appeared at 437 nm with two shoulders at 414 nm and 429 nm on the left side. Except that two shoulders are also appeared at 448 nm of violet peak emission region and 455 nm of blue peak emission region on the right side which commonly referred to ZnO nanorods characteristic peaks (Fig. 10a). We observed very high intense peaks for nanocomposites that completely differed from pure nanomaterials. A clear and strong peak observed at 420 nm with both left and right shoulder hump generated at 486 nm, 437 nm and 445 nm for CdS NWs doped Felix in compare to the luminescence spectra

of pure Felix (Fig. 10d. But, for ZnO NRs doped Felix the peak intensity is really very high and a sharp peak is observed at 422 nm with small hump on both sides in the region at 414 nm and 436 nm, illustrated in Fig. 10b.

With the application of excitation wavelength 425 nm, a sharp emission peak is noticed at 608 nm with two shoulder humps at 587 nm and 598 nm regions (Fig. 11c) for CdS NWs. Extreme high intense sharp peak maxima is shifted at 590 nm with two shoulder peaks at 581 nm and 597 nm on both sides due to pure ferroelectric liquid crystal (Felix) plotted in Fig. 11e. But, comparatively low intense sharp peak is observed at 610 nm with two shoulders on left side at 586 nm and 602 nm and another shoulder is noticed on right side at 617 nm for CdS NWs doped Felix depicted in Fig. 11d. With a gradual effect of increase of intensity, a clear and strong broad peak observed at 603 nm with no such shoulder peak clearly found for ZnO NRs green emission region, but a distinct extra peak observed at 610 nm shown in Fig. 11a. In addition, we observe that the green emission intensity at 520 nm is increased as the ZnO nanorods size increased (micrometer order after it annealed) and interestingly a sharp peak is observed at 603 nm with two tiny humps located clearly at 576 nm and 586 nm (Fig. 11b). The slight deviation of those luminescence peaks from our experimental value occurred due to those nanomaterials deposited on SiO_2 coated layer. While the UV emission corresponds to the near band-edge emission, the green emission peaks referred to as deep-level or trap-state emission. The green transition has been attributed to the singly ionized oxygen vacancy in ZnO and the emission results from the radiative recombination of a photo-generated hole with an electron occupying the oxygen vacancy [33]. The progressive increase of the green emission relative to the UV emission as the CdS nanowires diameter decreases rather than ZnO nanorods suggested that there is a greater fraction of oxygen vacancies in thinner nanowires.

4. Conclusions

In summary, we have suggested a simple route of fabricating different nano materials like ZnO and CdS on a large scale through hydrothermal technique. The experimental results revealed that the variation of different diameters of nanorods/nanowires of different materials changes its optical and dielectric properties drastically. In continuation with this overall investigation of our detailed experimental observation, we prepared SiO_2 coated thin film of thickness at the order of micrometer ranges, where several amount of Felix incorporated with CdS and ZnO nano materials by spin coating. Lastly we conclude that, an interesting comparative study of optical behavior and exclusive idea of nanostructures growth formation in ferroelectric liquid crystalline material host. The novel fabrication and simple methodology of high yield nanodoped liquid crystal (NDLC) techniques really impressible, easily operating to optoelectronics and display devices that may also be applied to industrial production.

Acknowledgments

The authors wish to thank the funding agency DST, Government of India provided the financial assistance with the sanctioned Project Number *SR/S2/CMP-0020/2009*. K. Pal is grateful to DST for providing him doctoral fellowship and U.N. Maiti is grateful to UGC for providing him Dr. D.S. Kothari post-doctoral fellowship. The authors are grateful to Prof. Tarak Das Basu, Department of Biophysics and Biochemistry, University of Kalyani for providing AFM facility.

References

[1] X. Duan, Y. Huang, R. Agarwal, C.M. Lieber, Nature 421 (2003) 241.
[2] M.S. Fuhrer, J. Nygard, L. Shih, M. Forero, Y.G. Yoon, M.S.C. Mazzoni, H.J. Choi, J. Ihm, S.G. Louie, A. Zettl, P.L. McEuen, Science 288 (2000) 494.
[3] Z.F. Ren, Z.P. Huang, J.W. Xu, J.H. Wang, P. Bush, M.P. Siegal, P.N. Provencio, Science 282 (1998) 1105.
[4] Y.N. Xia, P.D. Yang, Y.G. Sun, Y.Y. Wu, B. Mayers, B. Gates, Y.D. Yin, F. Kim, H.Q. Yan, Adv. Mater. 15 (2003) 353.
[5] D. Routkevitch, T. Bigioni, M. Moskovits, J.M. Xu, J. Phys. Chem. 100 (1996) 14037.
[6] D.S. Xu, Y.J. Xu, D.P. Chen, G.L. Guo, L.L. Gui, Y.Q. Tang, Adv. Mater. 12 (2000) 520.
[7] X.F. Duan, C.M. Lieber, Adv. Mater. 12 (2000) 298.
[8] C.J. Barrelet, Y. Wu, D.C. Bell, C.M. Lieber, J. Am. Chem. Soc. 125 (2003) 11498.
[9] C. Tang, S. Fan, M. Lamy de Chapelle, P. Li, H. Dang, Adv. Mater. 12 (2000) 1346.
[10] A.M. Morales, C.M. Lieber, Science 279 (1998) 208.
[11] E.M. Wong, P.C. Searson, Appl. Phys. Lett. 74 (1999) 2939.
[12] Z.W. Pan, Z.R. Dai, Z.L. Wang, Science 291 (2001) 1947.
[13] J.Y. Lao, J.Y. Huang, D.Z. Wang, Z.F. Ren, Nano Lett. 3 (2003) 235.
[14] J.Y. Lao, J.Y. Huang, D.Z. Wang, Z.F. Ren, Nano Lett. 2 (2002) 1287.
[15] C. Ye, G. Meng, Y. Wang, Z. Jiang, L. Zhang, J. Phys. Chem. B 106 (2002) 10338.
[16] J. Zhang, L.D. Sun, H.Y. Pan, C.S. Liao, C.H. Yan, New J. Chem. 26 (2002) 33.
[17] C. Pacholski, A. Kornowski, H. Weller, Angew. Chem. Int. Ed. 41 (2002) 1188.
[18] M. Okulska-Bozek, T. Prot, J. Borycki, J. Kedzierski, Liq. Cryst. 20 (1996) 349.
[19] T.P. Majumder, M. Mitra, S.K. Roy, Phys. Rev. E 50 (1994) 4796.
[20] T.P. Majumder, S.S. Roy, S.K. Roy, Phys. Rev. E 54 (1996) 2150.
[21] T. Ray, S. Kundu, T.P. Majumder, S.K. Roy, R. Dabrowski, J. Mol. Liq. 139 (2008) 35.
[22] K. Pal, U.N. Maiti, T.P. Majumder, S.C. Debnath, Appl. Surf. Sci. 258 (2011) 163.
[23] K. Pal, U.N. Maiti, T.P. Majumder, P. Dash, N.C. Mishra, N. Bennis, J.M. Oton, J. Mol. Liq. 164 (2011) 233.
[24] X. Ge, Y. Ni, H. Liu, Q. Ye, Z. Zhang, Mater. Res. Bull. 36 (2001) 1609.
[25] X. Guo-yue, W. Han, C. Chuan-wei, Nonferr. Metals Soc. China 16 (2006) 105.
[26] J.S. Jang, U.A. Joshi, J.S. Lee, J. Phys. Chem. C 111 (2007) 13280.
[27] Q.Q. Wang, G. Xu, G.R. Han, J. Solid State Chem. 178 (2005) 2680.
[28] R.A. Smith, Semiconductors, second ed., Cambridge, London, 1978.
[29] K. Rajeshwar, N.R. de Tacconi, C.R. Chenthamarakshan, Chem. Mater 13 (2001) 2765.
[30] S. Wang, S. Yang, C. Yang, Z. Li, J. Wang, W. Ge, J. Phys. Chem. B 104 (2000) 11853.
[31] K. Pal, T.P. Majumder, S.C. Debnath, S. Ghosh, S.K. Roy, J. Mol. Struct. 1027 (2012) 36.
[32] A. Mang, K. Reimann, St. Rűbenacke, Solid State Commun. 94 (1995) 251.
[33] K. Vanheusden, W.L. Warren, C.H. Seager, D.R. Tallant, J.A. Voigt, B.E. Gnage, J. Appl. Phys. 79 (1996) 7983.